Self-Assembled Plasmonic Nanogaps:

Enabling Early Detection of Biofilm Formation

Cuong Nguyen,[a] William J. Thrift,[a] Arunima Bhattacharjee,[a] Mahsa Darvishzadeh-Varcheie,[b] Filippo Capolino,[b] Allon Hochbaum,[a] and Regina Ragan[a]

[a]Department of Chemical Engineering and Materials Science and [b]Department of Electrical Engineering and Computer Science, University of California, Irvine
Irvine, California 92697, United States
rragan@uci.edu

***Abstract*— *Pseudomonas aeruginosa* is an opportunistic, biofilm-forming pathogen. *P. aeruginosa* produces pyocyanin, a secondary metabolite as part of its quorum sensing signaling system activated during biofilm formation. Self-organized plasmonic nanogaps provide enhancements to Raman scattering signals to achieve 10 ng/mL limit of detection of pyocyanin that enables early detection of biofilm formation. We report, for the first time, in-line biofilm detection in microfluidic channels as early as three hours from the onset of bacterial culturing and quantification spanning five-orders of magnitude of pyocyanin concentration during biofilm formation of PA14.**

Keywords*— *Colloids, self-assembly, surface enhanced Raman scattering, plasmonics, biofilms, metabolomics, quorum sensing, biosensor

I. INTRODUCTION

Pseudomonas aeruginosa is an opportunistic, biofilm-forming pathogen that is associated with contamination of medical devices, respiratory infections and one of the most common bacteria isolated in chronic wounds [1]. During biofilm formation, density-dependent gene expression is regulated; a mechanism called quorum sensing (QS). In the early phase, the expressed genes aggregate planktonic cells and start the production of extracellular polymeric substances (EPS) and QS signaling molecules [2]. Once developed, bacterial biofilms often exhibit resistance mechanisms such as efflux pumps, which specifically pump out antibacterial molecules [3] and can withstand up to 1000 times higher doses of antibiotics than their free floating planktonic counterparts [4]. While new antimicrobial strategies are being developed to combat antibiotic resistance, here we investigate a promising parallel strategy, sensing QS molecules for early detection of biofilm formation at a stage where antibiotic treatment has higher efficacy.

Among the many virulence factors and QS compounds that *P. aeruginosa* produces is pyocyanin [5], a redox active secondary metabolite which can act as a terminal signaling factor in the QS process. Surface enhanced resonance Raman scattering (SERRS) can be employed as a label free detection method since SERRS produces "molecular fingerprints" composed of the vibrational spectrum of molecules and pyocyanin exhibits a broad absorption band from 550 nm to 900 nm, in the range of the plasmon resonance of optical nanoantennas. SERS substrates often exhibit tradeoffs between uniformity of signal and intensity of the signal. Yet it is necessary to have both high and uniform enhancement factors across SERS substrates to reproducibly achieve low detection limits for two important reasons. First, at extremely low concentrations, pyocyanin will not be uniformly distributed across the surface. Hotspot sites will only be statistically populated with analyte molecules; thus uniformity of sites with high enhancement will lead to a higher probability that pyocyanin will reside in a hot spot and thereby enable lower detection limits. Second, when using machine learning to quantify pyocyanin concentration a large number of data sets are needed to achieve reliable quantification of pyocyanin concentration; i.e, hotspot uniformity across the surface will yield uniformity in SERRS signal when pyocyanin concentration is randomly distributed across the surface.

Large scale uniformity of SERS substrates is achieved here using a novel, hierarchical self-assembly approach for arranging Au nanospheres into oligomers, discrete clusters of nanospheres, with uniform nanometer gap spacings that are dictated by the chemical crosslinking agent used for assembly. This process can achieve a high yield of oligomers with gap spacing of 0.9 nm, consistent with the length of the anhydride bridge crosslinker. These oligomers exhibit an absorption band over 615 nm - 875 nm (full width half maximum). The range of the resonance is important to enhance both the incoming and Raman scattered light to maximize signal enhancements. Full wave simulations also show an electric field enhancement on the order of 600 in the hotspot region due to the narrow gap spacing in oligomers [6].

Here we show that by combining SERS substrates with machine learning algorithms, we are able to differentiate pyocyanin in the complex soup of biological media at concentrations down to 10 ng/mL and detect the presence of pyocyanin in biofilm cultures as early as 3 hours after culturing, earlier than other SERS based sensors. Self-assembly enables low cost fabrication of optical sensors coupled with low detection limits; these sensors will have significant impact in medical diagnostic applications in addition to early detection of biofilm formation when antibiotics have higher efficacy.

II. QUANTIFICATION OF PYOCYANIN DETECTION

A. Nanogap Fabrication

Nanogaps are formed between Au nanospheres that are assembled into oligomers on a chemically functionalized poly(styrene-b-methyl methacrylate) (PS-b-PMMA) diblock copolymer template. Hierarchical assembly combines long range, electrohydrodynamic (EHD) flow [7], and short range, chemical crosslinking, driving forces. Induced by an electric field in colloidal solution, EHD flow promotes lateral motion and close-packing of particles in colloid at the electrode surfaces, assembling transient close-packed structures. Resultant structures are typically imaged *in situ* using confocal microscopy making it difficult to understand assembly behavior at sub-100 nm dimensions. Here transient structures are frozen using EDC, a carbodiimide crosslinker, to form an anhydride bridge between the carboxylic acid ligands on Au nanospheres. This leads to uniform 1 nm spacings that lead to local enhancements of the electric field and provide enhancement of SERRS signals. A scanning electron microscopy image of Au oligomers is shown in Fig. 1(left).

B. Large-Area Uniformity of Surface Enhanced Raman Scattering Intensity

SERS measurements are conducted using a Renishaw InVia Raman Microscope system. A 785 nm continuous wave laser is chosen to excite near the plasmon resonance of Au nanoparticle assemblies as determined from electromagnetic simulations and ultraviolet-visible absorption measurements [6]. Approximately 150 µL of solution of interest is transferred onto SERS substrates and the measurements are acquired with laser power and acquisition time of 7.3 µW and 0.5 second, respectively. Fig. 1(right) displays the normalized SERS intensity of a benzenethiol vibration band, 1573 cm^{-1}, over a 100 µm x 100 µm area. The SERS intensity has a relative standard deviation (RSD) of 10.4%.

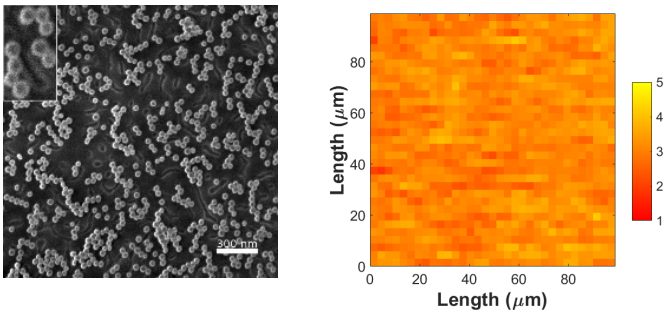

Fig. 1. (left) SEM image of self-assembled Au oligomers. (right) SERS map normalized SERS intensity of benzenethiol's 1573 cm^{-1} vibrational band.

Similar SERS substrates previously characterized report enhancement factor above 10^9 with RSD below 10% over 1 mm^2 using the same fabrication procedure [6]. These results demonstrate how assembly using EHD flow improves optical device performance as the contemporary state of the art SERS substrate have achieved variations of a factor of two (with enhancement of 10^7) [8]. The uniform SERS response with large enhancements over large area enables the use of these SERS substrates in device architectures. It also enables the acquisition of large datasets needed for statistical analysis for quantitative detection.

SERRS spectra of pyocyanin spiked in water from 100 ppt (fg/mL) to 100 parts per million (ppm; µg/mL) are shown in Fig. 2(left). Clear Raman bands at 552 cm^{-1}, 1353 cm^{-1}, 1602 cm^{-1}, and 1620 cm^{-1} are observed, highlighted in gray. A linear regime between 1 ppb and 10 ppm, consistent with Langmuir adsorption kinetics, is observed on the log-log dose-response curve of pyocyanin using normalized SERRS intensity at 552 cm^{-1}, as shown in Fig 2(right). Limit of detection was determined from the intensity at 552 cm^{-1} at the concentration where the signal from pyocyanin is one standard deviation above the noise level. The noise level is calculated by adding the mean background signal (DI water) at 552 cm^{-1} and three times the standard deviation of this signal. From this analysis, the LOD for pyocyanin was determined to be 100 ppt.

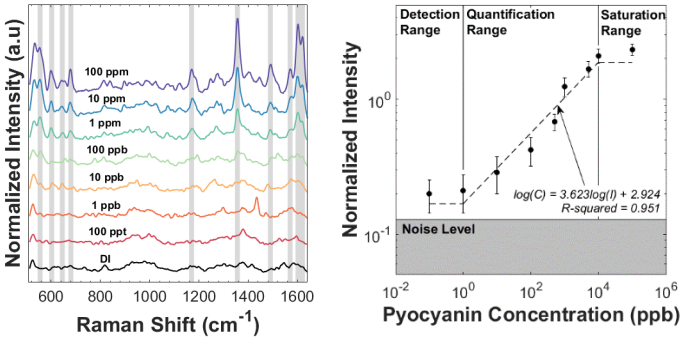

Fig. 2. (left) SERRS spectra of pyocyanin contrasted with blank spectra of DI water. Grey bars indicate dominant Raman bands of pyocyanin. (right) Normalized SERS intensity at 552 cm^{-1} dose-dependent response. Each point represents the average intensity across 150 spectra; error bars show standard deviation. The horizontal dashed line represents the calculated *Noise Level*.

C. Machine Learning Training Data

Use of a linear regression on a single Raman band, discussed in the prior section, allows for facile comparison with other SERS surfaces in the literature as it is widely used for quantitative calibration [9]. While this method is sufficient for pure analyte, it can lose sensitivity when other molecules are present in solution. Furthermore, it discards the remaining rich information in each spectrum and overlooks spectral variations. Here, we capitalize on the large-area uniform SERRS response of our surfaces and employ partial least square (PLS) analysis to quantify pyocyanin in more complex media. This allows for understanding how to differentiate between pyocyanin in the increased background noise of the biological media.

SERRS spectrum of pyocyanin spiked in LB media was collected to quantify pyocyanin in biological media. 400 spectra of LB media spiked with 100 ppt to 100 ppm pyocyanin were collected for each concentration; 380 were randomly chosen for calibration, and the remaining 20 for testing. LB media was used to emulate the environment of cell free conditioned medium. The model was then generated using the calibration set with 10 PLS components where RMSE cross validation is minimized. With the testing set, the model demonstrates accurate prediction between 1 ppb and 100 ppm, shown in Fig 3(left). Fitting a line with slope of 1 – representing perfect predictive capability – gives a R^2 value of 0.956. The quantification range for pyocyanin in LB media was thus determined to be 1 ppb to 100 ppm.

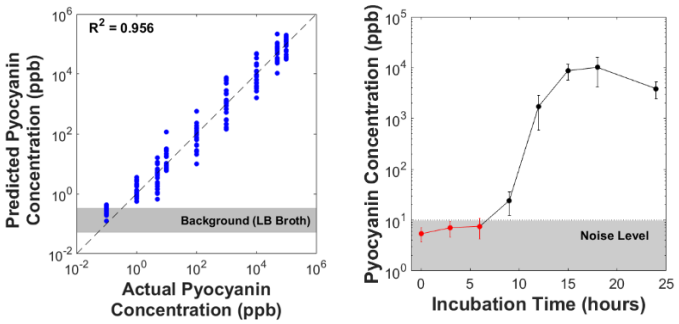

Fig. 3. (left) Pyocyanin concentration in LB broth predicted by PLS model . Pyocyanin can be quantified between 1 ppb and 10 ppm. (right) Pyocyanin concentration profile predicted by PLS model from SERRS spectra obtained at different time point of biofilm growth using in-line measurement procedure. Each data point represent the average from 200 spectra and error bars show standard deviation.

III. Monitoring Pyocyanin Production in PA14

A. Microfluidic Device Fabrication

The microfluidic device consists of two channels, one for the biofilm and the other for the SERS substrate. Micro-channels for biofilm were made by bonding the plasma-activated surfaces of PDMS with a glass slide. SERS micro-channels are made from SERS substrate and a glass slide separated by an adhesive spacer of 100 µm thickness (3M 415). Here, a commercial laser cutter (Epilog Fusion Laser Cutter) was employed to engrave channel design on the adhesive layer.

B. Biofilm Growth in Micro-channel

P. aeruginosa biofilms for in-line detection of pyocyanin were grown in the above microfluidic devices as previously described [10]. P. aeruginosa cells were seeded with no flow in the channels for 2 h. The fluid feed was then switched to sterile tryptone media and the outlet of the channel was connected to the SERS channel input. Media was pulled through the in-line detection device at 10 µL/h. SERRS spectra were then collected as described below.

C. In-line Detection of Biofilm Formation

Microfluidic channels were incorporated with SERS substrates to perform in-line detection of pyocyanin to monitor biofilm growth. Supernatant is delivered from a separate micro-channel to the sensing device. 200 SERS spectra were collected every 3 hours. Due to different growth media and SERS collection parameters, PLS regression was repeated on the appropriate calibration dataset to generate a suitable predictive model for the SERS spectra collected during biofilm growth (not shown). Here, PLS regression was able to quantify pyocyanin concentration after 9 h of biofilm growth, shown in Fig. 3(right). However, interestingly, 7.8% and 14.3% of the spectra at 3h and 6h, respectively, give pyocyanin concentration above the noise level. This fraction increases to 70.3%, 96.7%, and 100% for the subsequent time points. Investigation of individual spectra at 3h and 6h reveals clear pyocyanin Raman bands (not shown). This can be explained by the non-uniform distribution of pyocyanin on the substrate's surface at low concentrations. As mature biofilms exhibit increasing antibiotic resistance and tolerance, early detection – and hence early treatment – of a *P. aeruginosa* infection can potentially provide improvement for treatment efficacy and infection outcomes.

IV. Conclusion

In this work, the efficacy of chemically assembled SERS substrates were investigated for detecting pyocyanin as a signaling agent of biofilm formation. Driving assembly of Au nanopheres using EHD flow and EDC/S-NHS crosslinking chemistry produces a high density of oligomers with 1 nm gap spacings between nanospheres that provide large and uniform SERS enhancement factors. This yields a limit of detection of 100 ppt of pyocyanin in aqueous media and 10 ppb in complex media. Using PLS regression of SERRS data to quantify pyocyanin from cell-filtered supernatant in a microfluidic channel demonstrated detection of biofilm formation as early as 3 hours after culturing.

Acknowledgment

The authors acknowledge the National Science Foundation EECS- 1449397 for funding this work. The authors also acknowledge the use of the facilities within the Laser Spectroscopy Facility and the Laboratory for Electron and X-ray Instrumentation (LEXI) center at the University of California, Irvine. The authors would like to thank also Computer Simulation Technology (CST) of America, Inc. for providing CST Microwave Studio that was instrumental in this work.

References

[1] R. Serra *et al.*, "Chronic wound infections: the role of Pseudomonas aeruginosa and Staphylococcus aureus," *Expert Rev. Anti Infect. Ther.*, vol. 13, no. 5, pp. 605–613, May 2015.

[2] R. Kolter and E. P. Greenberg, "Microbial sciences: The superficial life of microbes," *Nature*, vol. 441, no. 7091, pp. 300–302, May 2006.

[3] S. M. Soto, "Role of efflux pumps in the antibiotic resistance of bacteria embedded in a biofilm," *Virulence*, vol. 4, no. 3, pp. 223–229, Apr. 2013.

[4] M. Malone, D. M. Goeres, I. Gosbell, K. Vickery, S. Jensen, and P. Stoodley, "Approaches to biofilm-associated infections: the need for standardized and relevant biofilm methods for clinical applications," *Expert Rev. Anti Infect. Ther.*, vol. 15, no. 2, pp. 147–156, Feb. 2017.

[5] J. C. Davies, "Pseudomonas aeruginosa in cystic fibrosis: pathogenesis and persistence," *Paediatr. Respir. Rev.*, vol. 3, no. 2, pp. 128–134, Jun. 2002.

[6] W. Thrift *et al.*, "Bridging the Gap between Crosslinking Chemistry and Directed Assembly of Metasurfaces Using Electrohydrodynamic Flow," *ArXiv160906964 Cond-Mat Physicsphysics*, Aug. 2016.

[7] W. D. Ristenpart, I. A. Aksay, and D. A. Saville, "Electrically Driven Flow near a Colloidal Particle Close to an Electrode with a Faradaic Current," *Langmuir*, vol. 23, no. 7, pp. 4071–4080, Mar. 2007.

[8] K. N. Kanipe, P. P. F. Chidester, G. D. Stucky, and M. Moskovits, "Large Format Surface-Enhanced Raman Spectroscopy Substrate Optimized for Enhancement and Uniformity," *ACS Nano*, vol. 10, pp. 7566–7571, Aug. 2016.

[9] C. Srichan *et al.*, "Highly-Sensitive Surface-Enhanced Raman Spectroscopy (SERS)-based Chemical Sensor using 3D Graphene Foam Decorated with Silver Nanoparticles as SERS substrate," *Sci. Rep.*, vol. 6, p. 23733, Mar. 2016.

[10] A. Bhattacharjee, M. Khan, M. Kleiman, and A. I. Hochbaum, "Effects of Growth Surface Topography on Bacterial Signaling in Coculture Biofilms," *ACS Appl. Mater. Interfaces*, vol. 9, no. 22, pp. 18531–18539, Jun. 2017.